Nanotomography

Robert Magerle*
Physikalische Chemie II, Universität Bayreuth, D-95440 Bayreuth, Germany
(Received 4 October 1999)

Scanning probe microscopy (SPM) can be expanded to volume imaging. As an example, the core of a dislocation within the three-dimensional (3D) spatial microdomain structure of poly(styrene-*block*-butadiene-*block*-styrene) was imaged with ≈10 nm resolution. The specimen was eroded step by step and its chemical composition in layers beneath the original surface was imaged with SPM. Similar to computed tomography, the 3D distribution of polystyrene and polybutadiene was reconstructed from a series of images. This approach might provide a simple means for *real-space* volume imaging with nanometer and even atomic resolution of various materials and physical properties.

PACS numbers: 61.16.Ch, 61.41.+e, 61.72.Lk, 81.70.Jb

Imaging is pervasive in science and new insight into self-organization of matter is often triggered by new imaging techniques. Despite the vast number of condensed matter systems with spatial structures on submicron and smaller scales—ranging from alloys and composite materials over submicron electronic devices to cells and viruses—only very few methods are available for 3D imaging of such small objects. In most cases scattering methods are not applicable due to lack of translatorial symmetry. Until now, the only *real-space* volume imaging methods covering the nanometer scale are reconstruction from serial sections using transmission electron microscopy [1,2] and electron tomography [3]. With both of these methods the electron density is imaged primarily; also with both, the specimens must be transparent to electrons and machinable into some 10 nm thick slices. As a result, very few specimens, usually biological, can be studied in such a fashion. For other specimens, such as submicron devices or metallic alloys, and for imaging other properties, such as the doping density of a semiconductor, appropriate methods for high-resolution 3D imaging are missing.

Since 1982 the scanning tunnelling microscope (STM) [4] and its offspring have been revealing individual atoms and molecules on crystal surfaces. With other members of the family of scanning probe microscopies (SPM), almost every physical property has been measured on an unprecedentedly fine scale. However, only the surface of specimens can be studied, which is considered to be a serious limitation of SPM.

Classical optical microscopy and electron microscopy are limited in a similar manner since only the surface or thin slices of specimens can be imaged. A common approach to overcome this limitation is reconstruction from serial sections. In classical optical and transmission electron microscopy, the specimen is physically cut into a series of thin slices. With confocal laser scanning microscopy, computed tomography, and magnetic resonance imaging, on the other hand, images of thin slices are obtained nondestructively by suitable measurement techniques. In either case, a 3D volume image is reconstructed from a series of two-dimensional (2D) images. In his pioneering work in 1876, Gustav Born cut wax plates after microscope images which he then put together manually [5]. Nowadays, this task is accomplished with the help of computers and data visualization software.

In this Letter, a general procedure for volume imaging with SPM is presented. The method is based on the principle of reconstruction from serial sections; however, instead of sectioning, ultrathin layers are stepwise removed from the specimen and the sample's surface is imaged with SPM after each removal step (Fig. 1). From the series of images, the 3D distribution of the physical property imaged with SPM is reconstructed. This approach is not new; indeed it is the operating principle of depth profiling with surface sensitive techniques such as secondary ion mass spectroscopy [6]. With these techniques, however, depth resolution is limited by the roughness r of the specimen, which is either intrinsic to the (heterogeneous) specimen or induced by the etching process [7]. In either case, signals from different depths of the original specimen are detected simultaneously, which deteriorates depth resolution and limits the approach to very homogenous materials. In contrast, the method presented here is *not* limited by roughness since SPM can establish the surface topography simultaneously with the sample properties under study. Therefore each image is a curved surface and depth resolution is limited only by the local distance d

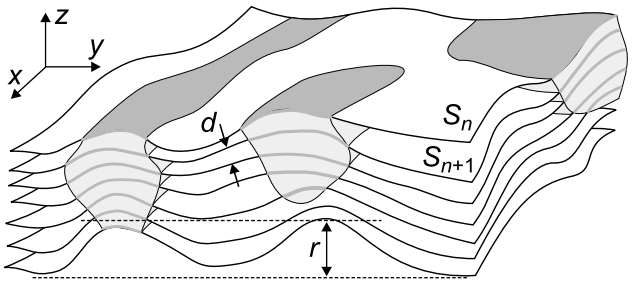

FIG. 1. Schematic illustration of the principle of volume reconstruction from a series of scanning probe microscopy images. In general, the surfaces S_n on which the property $P_n(S_n)$ is measured are curved.

between two adjacent surfaces and the surface sensitivity of the employed SPM technique as indicated in Fig. 1 [8].

This approach might provide a simple means for nanometer (and even atomic) resolution *real-space* volume imaging of various materials and physical properties. With the success of SPM in mind, *volume imaging* by SPM promises new insights into the physics of condensed matter on a nanometer scale.

To demonstrate the feasibility of this idea, the 3D microdomain structure of the triblock copolymer poly(styrene-*block*-butadiene-*block*-styrene) (SBS) was imaged with ≈10 nm resolution. TappingMode™ scanning force microscopy (SFM) was used for mapping the distribution of polystyrene (PS) and polybutadiene (PB); plasma etching for stepwise erosion of the specimen. The data reveal the 3D morphology of the core of a transverse edge dislocation in the SBS microdomain structure of hexagonally ordered PS cylinders.

SBS is a prototype of a modern synthetic rubber and widely used as thermoplastic elastomer. At room temperature, the PS and PB blocks are immiscible and phase separate into microdomains which form a regular superstructure with characteristic lengths given by the size of the molecules. This behavior is typical for block copolymers composed of two or more blocks of immiscible polymers and is well understood [9,10]. In practice, block copolymers are "polycrystalline" with numerous imperfections in the microdomain structure. However, due to lack of suitable imaging techniques, very little is known about the structure of these defects [11,12] and their relationship to the mechanical [13,14] and transport [15] properties of block copolymers.

The SBS used in this work was obtained from Polymer Source Inc. and the PS, PB, and PS blocks had weight averaged molecular weights M_w of 14 000, 73 000, and 15 000, respectively, and a polydispersity of 1.02. This molecular architecture causes the PS blocks to self-organize into cylinders of about 24 nm diameter embedded into a PB matrix. Viewed along their long axes, the cylinders form a hexagonal lattice with a mean distance of 42 ± 1 nm between two next-nearest cylinders [9]. To simplify the experiment, a 140 ± 4 nm thick SBS film was prepared by spin-casting a 2 wt % solution of SBS in toluene onto a cleaned silicon wafer about 1 cm^2 in size. For equilibration and long range ordering of the SBS microdomain structure, the thin film specimen was treated overnight in toluene vapor. After this procedure PS cylinders tend to orient parallel to the film plane [16].

The lateral distribution of PS and PB near the film surface can be imaged with SFM operated in TappingMode™ when a phase image $\varphi(x, y)$ is recorded in addition to the surface topography $z(x, y)$. The phase image reflects lateral differences in the mechanics of the tip-sample interaction which differs considerably between PS and PB due to the large difference in their glass transition temperatures T_g. At room temperature, PS ($T_g \approx 100\,^{\circ}C$) is hard and PB (with 1,4-addition $T_g \approx -105\,^{\circ}C$) is soft. Therefore the phase image can be interpreted as a high-resolution map of the near-surface distribution of PS and PB [17]. After film preparation, the phase image shows a stripe pattern, indicating that the PS cylinders are oriented parallel to the film surface.

For volume imaging, 7.5 ± 0.2 nm (on average) thick layers of the block copolymer were successively removed by plasma etching and TappingMode™ SFM images were taken (with a Dimension 3100 from Digital Instruments) after each etching step. A spot was chosen with characteristic landmarks within and nearby the imaged area which help in finding the same spot again after *ex situ* plasma etching. For plasma etching, the specimen was placed in a Harrick PDC-32G Plasma Cleaner which was then operated with air at 1.5 ± 0.1 mbar pressure and 60 W rf power for 20 s.

After 13 etching steps and removal of an approximately 100 nm thick layer from the initial film surface a stripe pattern is still visible in the phase image [Fig. 2(h)]. In the corresponding topography image [Fig. 2(a)], a similar stripe pattern is present. This is attributed to the somewhat higher etching rate of PB [18] which causes the PS-rich domains to protrude about 1–2 nm over the PB-rich areas after etching. Between the bottom left and the top right part of the phase image shown in Fig. 2(h), there is a region (1) (marked by dashed lines) where the distance between bright stripes is only half of the distance in the other parts of the image. The position and the shape of this region coincide with the slope between the respective areas visible in the corresponding topography image [Fig. 2(a)]. The top right corner is about 17 ± 2 nm higher than the bottom left one. This height difference compares well with the center-to-center distance of two adjacent layers of PS cylinders. Based on this finding, the phase image shown in Fig. 2(h) can be interpreted as a curved cross section through the original SBS film. This cross section crosses one layer of PS cylinders in the top right corner of the image and the adjacent lower layer of PS cylinders in the bottom left part of the image.

A series of topography and phase images of the same spot after successive etching steps is displayed in Fig. 2. A stripe pattern is visible in all images; however, the region where the distance between two bright stripes is only half the distance between the PS cylinders is changing in Figs. 2(h)–2(n). This is consistent with the interpretation of Figs. 2(a) and 2(h) given above. After each etching step, the exposed surface is crossing a layer of PS cylinders in another region of the image. Finally, after seven more (20 in total) etching steps, the silicon substrate is exposed in parts of the imaged area [Figs. 2(g) and 2(n)]. The series of images can be viewed as a series of curved cross sections through the original sample at an average distance $\langle d \rangle = 7.5 \pm 0.2$ nm. The phase images $\varphi_n(x, y)$ [Figs. 2(h)–2(n)] can be interpreted as maps of the PS-to-PB ratio at the exposed sample surface

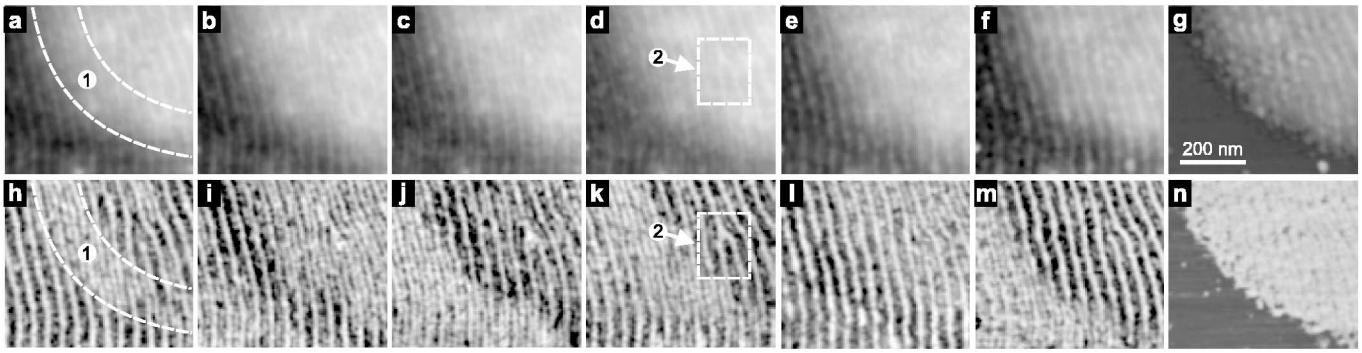

FIG. 2. Series of TappingMode™ SFM images from a thin SBS film. Topography [(a)–(g)] and the corresponding phase images [(h)–(n)] are shown. Between each pair of images a 7.5 ± 0.2 nm (on average) thick layer has been removed from the sample by plasma etching. For (1), see text. Region (2) is displayed as a 3D image in Fig. 3.

after the nth etching step. Bright (dark) areas indicate a high (low) phase which corresponds to a high PS (PB) volume fraction. Together with the corresponding topography images $z_n(x, y)$ [Figs. 2(a)–2(g)] describing the curved surfaces, they can be combined to phase maps $\Phi_n[x, y, z_n(x, y) - n\langle d\rangle]$ which are defined on curved surfaces S_n, as indicated in Fig. 1.

From this series of phase maps Φ_n a volume image of the PS-to-PB ratio can be reconstructed. Since the SFM images cannot be taken exactly at the same spot, the images of a series have to be aligned (registered) prior to volume reconstruction. Image registration is widely used in computed tomography, magnetic resonance imaging, and other areas of science [19]. In this work, the correlation coefficient between two subareas of neighboring topography images was maximized which enables alignment of two images with subpixel precision. After image alignment, a volume map of the phase information can be reconstructed since the effective phase Φ is sampled at the points $[x, y, z_n(x, y) - n\langle d\rangle]$ spanning a regular mesh within the original specimen. To achieve the same contrast in all phase images, each phase image was normalized such that the mean phase is zero and the standard deviation of the normalized phase equals 0.33 in all images.

A visualization of the 3D phase distribution is shown in Fig. 3 where the isosurface enclosing the volume with normalized phase >0.11 was reconstructed from the series of topography and phase images displayed in Fig. 2. The enclosed volume can be interpreted as PS cylinders within a $200 \times 160 \times 45$ nm^3 large portion of the SBS film. The cylinders are well resolved in the xy plane as well as in the z direction. The hexagonal lattice of PS cylinders is found to be compressed in the z direction in agreement with Ref. [16], where SBS films have been prepared with a similar toluene vapor treatment procedure. The undulations and protrusions of the cylinders are believed to be an artifact caused by the discreteness of the raw pixel data. It is noteworthy that the diameter of a single cylinder (24 nm) corresponds to the width of only four pixels in the original SFM images and that the tip radius ($\approx$10 nm) is of comparable size. Figure 3 demonstrates that volume images can indeed be obtained with SPM. A spatial resolution comparable with the intrinsic high lateral resolution of the employed SPM technique is achieved in all three dimensions. In the present case, the resolution is limited only by the tip radius. With sharper tips a higher spatial resolution could be achieved.

In the center of Fig. 3, a branching of a PS cylinder is visible which in Figs. 2(j) and 2(k) appears as a bifurcation. Such bifurcations are often observed in transmission electron micrographs of thin sections of SBS and other block copolymers with cylinder morphology [9,10,12]; however, these images are 2D projections of 3D structures. In contrast, Fig. 3 is a volume image

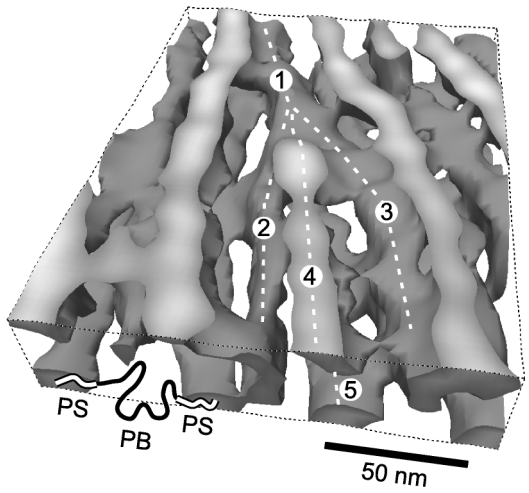

FIG. 3. 3D image of the isosurface enclosing the volume with normalized phase >0.11 reconstructed from the series of phase and topography images shown in Fig. 2. This can be interpreted as PS cylinders within a $200 \times 160 \times 45$ nm^3 large portion of the SBS film. In the center, a branching of a PS cylinder (1) into four other PS cylinders (2)–(5) is displayed which is the core of a dislocation line in the SBS microdomain structure of hexagonally ordered PS cylinders. For size comparison and illustration of the molecular structure of the material, a SBS molecule bridging two PS domains is sketched.

and a detailed inspection of the isosurface from different viewpoints reveals that the PS cylinder (1) is not only branching into the two cylinders (2) and (3) lying in a common plane with cylinder (1) but at the branching point is additionally connected with the two cylinders (4) and (5) lying in the two neighboring planes of PS cylinders. This unexpected result demonstrates that *real-space* volume imaging with SPM offers new information about structures on the nanometer scale which would be difficult (if not impossible) to obtain with existing techniques. Electron tomography [3,20], for instance, would require staining and assumptions of a specific symmetry of the specimen for employing noise reducing image processing techniques. Further studies are needed to establish whether or not this particular type of branching is a common kernel of a transverse edge dislocation line in the microdomain structure of hexagonally packed cylinders in SBS and other block copolymers.

These results demonstrate that volume imaging with SPM is possible. This method enables high-resolution *real-space* volume imaging of material properties that can be imaged only with such a high spatial resolution by SPM. Furthermore, it enables volume imaging of specimens that either cannot be sectioned into thin slices or do not provide suitable contrast for electron microscopy. A key feature of the presented method is that both the surface properties P_n under study as well as the topography S_n are acquired with SPM and that the sections $P_n(S_n)$ are defined on curved surfaces S_n in general. This means that neither homogenous etching nor flat sample surfaces are required for the method, ensuring its application to a large class of heterogeneous and thereby interesting materials, such as composites, alloys, and submicron electronic devices.

All of these possibilities promise new insights into condensed matter on a nanometer scale. In the present case of the core of a dislocation in the microdomain structure of SBS (Fig. 3), the complex 3D structure of a self-organized assembly of SBS macromolecules was imaged with submolecular resolution. Starting from surfaces prepared by freeze fracture the method could shine new light on the ultra-structure of cells and viruses. Furthermore, submonolayer etching [21] and growth [22] of crystalline materials has been imaged *in situ* with STM with atomic resolution. Therefore it appears feasible that the volume structure of a metallic alloy or a doped semiconductor can be reconstructed atom-by-atom in real space. Finally, the method has the potential of being fully automated since both fully automated etching as well as SPM imaging are state of the art semiconductor technology today.

This work was partly supported by the Deutsche Forschungsgemeinschaft. The author thanks G. Krausch, M. Konrad, and A. Knoll for stimulating discussions and M. Geoghegan for help with the manuscript.

*Electronic address: robert.magerle@uni-bayreuth.de

[1] F. S. Sjöstrand, J. Ultrastruct. Res. **2**, 122 (1958).
[2] W. A. Gaunt and P. N. Gaunt, *Three Dimensional Reconstruction in Biology* (Pitman Medical, Kent, 1978).
[3] J. Frank, *Three-dimensional Electron Microscopy of Macromolecular Assemblies* (Academic Press, San Diego, 1996).
[4] G. Binnig, H. Rohrer, C. Gerber, and E. Weibel, Phys. Rev. Lett. **49**, 57 (1982).
[5] G. Born, Morphologisches Jahrbuch **2**, 578 (1876); Archiv für mikroskopische Anatomie **22**, 584 (1883).
[6] K. Wittmaack, in *Sputtering by Particle Bombardment III,* edited by R. Behrisch and K. Wittmaack (Springer-Verlag, Berlin, 1991) p. 161.
[7] G. Carter, B. Navinšek, and J. L. Whitton, in *Sputtering by Particle Bombardment II,* edited by R. Behrisch (Springer-Verlag, Berlin, 1983), p. 231.
[8] A PCT patent application for this method has been filed at the German Patent Office.
[9] A. Keller and J. A. Odell, in *Processing, Structure and Properties of Block Copolymers,* edited by M. J. Folkes (Elsevier, London, 1985), p. 29.
[10] For recent reviews, see J. W. Hamley, *The Physics of Block Copolymers* (Oxford University Press, Oxford, 1998); F. S. Bates and G. H. Fredrickson, Annu. Rev. Phys. Chem. **41**, 525 (1990).
[11] S. P. Gido and E. L. Thomas, Macromolecules **27**, 849 (1994).
[12] L. H. Radzilowski, B. L. Carvalho, and E. L. Thomas, J. Polym. Sci. B, Polym. Phys. **34**, 3081 (1996).
[13] R. J. Albalak and E. L. Thomas, J. Polym. Sci. B, Polym. Phys. **31**, 37 (1993).
[14] J. Hahm *et al.,* J. Chem. Phys. **109**, 10 111 (1998).
[15] D. J. Kinning, E. L. Thomas, and J. M. Ottino, Macromolecules **20**, 1129 (1987).
[16] G. Kim and M. Libera, Macromolecules **31**, 2569 (1998); **31**, 2670 (1998).
[17] S. N. Magonov *et al.,* Surf. Sci. **389**, 201 (1997).
[18] M. Konrad, Diplomarbeit, Universität Bayreuth, 1999.
[19] L. G. Brown, ACM Computing Surveys **24**, 325 (1992).
[20] R. J. Spontak, M. C. Williams, and D. A. Agard, Polymer **29**, 387 (1988).
[21] For a review, see K. Itaya, Prog. Surf. Sci. **58**, 121 (1998).
[22] See, e.g., B. Voigtländer, M. Kästner, and P. Šmilauer, Phys. Rev. Lett. **81**, 858 (1998).